Anticancer activity of CT-p19LC, a synthetic peptide derived from the bacterial protein azurin

Lígia Patrícia Fonseca Coelho
iBB – The Institute for Bioengineering and Biosciences
Instituto Superior Técnico
Av. Rovisco Pais 1, 1049-001 Lisboa

Abstract

Several cationic peptides have recently been shown to display anticancer activity through a mechanism that usually requires the disruption of cancer cell membranes. In this thesis project, we designed a 19-residue presumptive ACP_{AO}, designated CT-p19LC, using as template CT-p26, a 26-residue peptide derived from the protein azurin. Produced by *Pseudomonas aeruginosa,* the bacteriocin azurin has been explored regarding its multi-target anticancer potential. It was demonstrated in previous studies that azurin deleterious effect at the membrane level of epithelial cancer cell lines is closely related to a phenylalanine residue in position 114 near its C-terminal. Thus, CT-p26, a peptide which comprises the azurin region from 94-120 amino acids was tested against breast and lung cancer cell lines demonstrating a significant cytotoxic effect. In the present study we took advantage of appropriate bioinformatics peptide optimization tools and originated CT-p19LC, a shorter peptide with point residue alterations with higher hydrophobicity, positive net charge and improved solubility. Consequently, *in vitro* MTT cell proliferation assays proved CT-p19LC is active against A549, MCF-7, HT-29 and HeLa cell lines treated in different doses whereas the cytotoxicity toward noncancerous cells such as MCF-10A and 16HBE14 is low. Membrane order assay with Laurdan's probe along with confocal microscopy gave quantification data which may support the intended mechanism of action at the cell's membrane level, although alternatives are also discussed. Finally, CT-p19LC appears to enhance erlotinib antincancer action in A549 lung cancer cells. Consequently, this work shows that levels of EGFR are disturbed by the treatment of CT-p19LC which may represent the first clue of the cell target of this newly design peptide and be the foundation for future studies.

Key words: Anticancer peptide, azurin, peptide-based drug development, *in silico,* chemotherapeutics, drug resistance

Introduction

Anticancer peptides, or ACPs, are small peptides with lengths reported between 5 to 40 amino acids, a molecular mass less than 10 kDa and a positive net charge at physiological pH. Structurally, ACPs have either α-helix (α-ACPs) or β-sheet (β-ACPs) conformation but some linear and extended structures have already been reported (Hoskin & Ramamoorthy 2008). It is common to find ACPs rich in R, K and P which are hydrophobic amino acids but H and W are also likely to be present (Sanchez-Navarro et al. 2017).

It has been established that tumor cells are up to 50 times more sensitive to lytic peptides than normal cells (Leuschner 2005). Regarding selectivity, ACPs can be classified in two broad categories. The first category contains the group of ACPs (ACP_{AO}) which is active against microbial cells and cancer cells while not being active against healthy mammalian cells. The second one includes ACPs (ACP_T) that are cytotoxic for bacteria and mammalian cells (Gaspar et al. 2013).

The reason behind ACP_{AO} selectivity is still a controversial topic however some conclusions are evident. Cancer and normal mammalian cells have a number of confirmed differences that are considered responsible for this selectivity phenomenon. The most described differences are membrane-based more exclusively regarding membrane net negative charge and abnormal fluidity due to change on cholesterol profile which characterizes malignant cells in contrast with healthy mammalian cells (Harris et al. 2011).

Interactions between ACPs and non-malignant mammalian cells are not favored due to the zwitterionic effect present in the membrane of these cells which confers an overall neutral nature. On the contrary, neoplastic cells carry a typical negative net charge due to an abnormal expression of anionic molecules such as phosphatidyl serine (Hoskin & Ramamoorthy 2008; Gaspar et al. 2013).

Regarding fluidity, there is evidence suggesting that cholesterol confers protection to non-malignant cells from the action of α-ACP_{AO} by blocking its access. Indeed, it was

found that the presence of lipid rafts rich in cholesterol can be a key factor on differentiating the action and effect of both ACP_{AO} and ACP_T which can also explain their different effect in diverse cancer cell lines depending on their nature of lipid raft constitution (Li et al. 2006)

Membrane disruption is probably the most studied ACP effect in malignant cells. Membranolytic peptides are proved to target different membrane components contributing to their selectivity. Also, their ability to pore formation and targeting may be intimately related to the peptides structure (Teixeira et al. 2012; Gaspar et al. 2013). Consequently, ACPs are also proved to adopt either a bioactive helical conformation at the cell surface or β-sheet structure preceding the engagement with the membrane. Besides structure, characteristics as positive net charge and presence of hydrophobic residues in high concentrations are also key factors for the membranolytic effect to occur and for the specificity towards cancer cells.

Apart from the plasmatic membrane, also other biomembranes can suffer the effects of membranolytic peptides. Cancer cells which suffer the action of lytic peptides in their mitochondria may initiate the signaling pathway of apoptosis. In situations where the plasmatic and/or mitochondrial membrane is too disrupted, the necrosis mechanism is triggered.

Azurin, expressed in the opportunistic human pathogen *Pseudomonas aeruginosa,* is a small cooper-binding electron transfer protein derived from the cupredoxin family that has demonstrated multi-target anticancer activity *in vitro* and *in vivo* (Punj et al. 2004; Bernardes et al. 2016). This protein is composed by 128 amino acids (14 kDa) and comprises eight antiparallel-strands connected by four loops linked by a disulfide bridge (Yamada et al. 2004; Fialho et al. 2016) and azurins' many different domains may be the reason for its different ways of targeting cancer cells and subsequently affect them.

In fact, azurin has been proved to enhance the anticancer activity of chemotherapeutical drugs such as doxorubicin and paclitaxel which provoke DNA damage (Bernardes et al. 2017 submitted) by turning the cancerous membranes more vulnerable to let anti-DNA chemotherapeutical drugs to perform. Also, other drugs which also target membrane components such as gefitinib and erlotinib are also proved to have its anticancer effect enhanced when in combination with azurin (Bernardes et al. 2016).

If in one hand p28 seems to be linked to azurins capacity of p53 targeting in another hand a recent study of Bernardes et al. 2017 (submitted) has shown significant evidence that a specific region near azurin's C-terminal extremity is essential to cancer cells' plasmatic membrane's targeting and penetration. In assays where azurin WT was compared to azurin F114A, significant data showed that the aromatic properties of F residue in azurin's 114 position are key to the membrane-targeting anticancer potential of this cupredoxin since its substitution for an A residue showed a clear decrease in the cytotoxic capacity of this mutant against cancer cells when comparing with the wild-type. In all the used concentrations, azurin F114A has a reduced entry capacity when compared to the azurin WT, thereby suggesting that this hydrophobic residue might play a role in the first recognition steps between azurin and *caveolae*, and that this interaction is probably critical to the entry of this bacterial protein in cancer cells. In addition, upon treatment with F114A azurin the effect in the lipid rafts seemed less accentuated which suggested that F114A azurin has poor penetration capacity in cancer cells. Also, it suggested that this hydrophobic domain of azurin is vital for its entry and the disruption of *caveolae* in the membranes of cancer cells (Bernardes et al. 2017 submitted).

With that in mind, a peptide designed from the C-terminal domain of azurin comprising F residue in the 114 position was synthesized and named CT-p26 and subsequently tested showing promising bioactivity against tumor cell lines.

Materials and methods

In silico analysis

Azurin protein sequences from all considered species in the query of the study were obtained from NCBI - National Center for Biotechnology Information (https://www.ncbi.nlm.nih.gov/) and aligned using standard protein blast tool (blastp) from the same source (https://blast.ncbi.nlm.nih.gov/Blast.cgi).

Peptide optimization was performed by two different bioinformatic tools. The first predictive tool was the peptide algorithm AntiCP from the Institute of Microbial Technology in India (http://crdd.osdd.net/raghava/anticp/). The second predictive tool was the Antimicrobial peptide database and its incorporated algorithm (http://aps.unmc.edu/AP/main.php). Innovagen™ peptide property calculator algorithm was used to predict the solubility potential of the query peptides (http://pepcalc.com).

For both peptide optimization algorithms and Innovagen's calculator, the input was the FASTA sequence of CT-p26 and the comparable 26 residue-portion from all other different azurins and afterward the FASTA sequence of the shortened versions.

Peptides

Within the domain of this work, two peptides (CT-p19 and CT-p19LC) were designed and their synthesis was ordered from Pepmic Co., Ltd. Lyophilized samples of CT-p19 and CT-p19LC was dissolved in 10 mM phosphate buffer (pH 7.4).

In addition, synthesis of CT-p26 and p28 were ordered from Pepmic Co., Ltd, and were dissolved in PBS – Phosphate buffer saline (pH 7.4).

Cell culture

Human epithelial cancer cell lines A549 (lung), HeLa (cervix), HT-29 (colorectal) and MCF-7 (breast) were obtained from ECACC (European Collection Of Authenticated Cell Cultures). They were maintained in DMEM-Dulbecco's Modified Eagle Medium (Gibco® by Life Technologies), supplemented with 10% of heat-inactivated Fetal Bovine Serum (Gibco® by Life Technologies), 100 IU/ml penicillin and 100 mg/ml streptomycin (PenStrep, Invitrogen). Human bronchial cell culture 16HBE14 was grown in MEM without Earls salts supplemented with 10% of Fetal Bovine Serum, 1% of L-glutamine and 10000 U/ml penicillin and 10000 mcg/ml streptomycin (PenStrep, Invitrogen). Human mammary gland cell line MCF-10A was cultured in MBEM (Lonza Co.). The culture conditions for all

cell lines were 37°C in a humidified chamber containing 5% of CO_2 (Binder CO_2 incubator C150).

MTT cell proliferation assay

Solo assays: MTT [3-(4,5 dimethylthiazol-2-yl-2,5 tetrazolium bromide)] assays were used to determine the viability of human A549 (lung), HeLa (cervix), HT-29 (colorectal) and MCF-7 (breast) adenocarcinoma cells as also 16HBE14 non-cancer bronchial cells and MCF-10A non-cancer breast cells exposure to the effects of azurin's peptides CT-p26, p28 or CT-p19 and CT-p19LC. Cancer cell lines were seeded in 96-well plates (Orange Scientific), in 3x replicates per well, at a density of 10^4 cells per well and were left to adhere and grow overnight in a CO_2 incubator (5%) at 37°C. The 16HBE14 and MCF-10A cells were seeded in 96-well plates (Orange Scientific), in 3x replicates per well, at a density of $7{,}5x10^4$ and $4{,}5x10^4$ cells per well, respectively, and were left to adhere and grow in the same conditions. In the next day, medium was collected and cells were treated with concentrations from 0 µM to 100 µM of the different peptides and were left for 48 h in the same growth conditions.

Combination assays: Lung A549 cancer cells were seeded in 96-well plates (Orange Scientific), in 3x replicates per well, at a density of 10^4 cells. After 24 h, medium was changed and fresh CT-p19LC, erlotinib (Santa Cruz), a combination of both or an identical volume of media with buffer were added and were left for 72 h in the same growth conditions.

After this time, 20 µL of MMT reagent (5 mg/ml) was supplemented to each well and incubated for 3.5 hours. The reaction was stopped by the addition of 40 mM HCl in isopropanol (150 µL). MTT formazan formed was spectrophotometrically read at 590 nm in a 96-well plate reader (SpectroStarNano, BMG LABTECH). Untreated cells were used as control, in order to determine the relative cell viability of treated cells.

Two-photon excitation microscopy – GP determination

The human A549 (lung), HeLa (cervix), HT-29 (colorectal) and MCF-7 (breast) adenocarcinoma cells were cultured on µ-Slide 8 well glass bottom chambers (ibidi®) with $5x10^4$ cells and treated with CT-p19LC (20 µM). After 2 h, medium was collected and cells were washed twice with PBS. After that, medium was renewed containing 5 µM of Laurdan's and the cells were incubated in a CO_2 incubator at 37°C for 15 min (Binder CO_2 incubator C150). Untreated cells were the control condition.

Samples were examined on a Leica TCS SP5 (Leica Microsystems CMS GmbH, Mannheim, Germany) inverted microscope (model no.DMI6000) with a 63× water (1.2-numerical-aperture) apochromatic objective. Two photon excitation data were obtained by using Leica TCS SP5 inverted microscope with a titanium-sapphire laser as the excitation light source. The excitation wavelength was set to 780 nm and the fluorescence emission was collected at 400–460 nm and 470–550 nm to calculate the GP images. Laurdan's GP images were obtained through homemade software based on a MATLAB environment.

Protein extraction and Western blot

The A549 cancer cells cultured in 6-well plates were serum-starved for 24 h prior to treatment with 20 µM of CT-p19LC for 2 h. EGFR signalling was stimulated by the addition of EGF (50 ng/mL), for 30 minutes. Non-stimulated cells represent control. All incubation time was at 37ºC in a 5% CO_2 atmosphere. For protein extraction the wells were washed twice with PBS 1x. Cell lyses was achieved using 100 µL of Catenin Lysis Buffer (CLB; 1% Triton X-100, 1% Nonidet-P40 in PBS) supplemented with 1:7 proteases inhibitor (Roche Diagnostics GmbH) and 1:100 phosphatases inhibitor (Cocktail 3, Sigma Aldrich) for 10 minutes at 4°C. The cells extracts were scratched, collected and vortexed three times (10 seconds each), centrifuged (14000 rpm, 4°C, 10 min; B. Braun Sigma-Aldrich 2K15) and the pellet was discarded, collecting the supernatant containing proteins.

The samples were quantified by a Quantification Protein Kit (Bradford, BioRad). The determination of the total protein concentration, per sample, was achieved through the use of a calibration curve, on which were used the absorbance values of standard samples of bovine serum albumin (BSA), whose concentrations are known (provided by the kit). Final quantification of 40 µg (EGFR phosphorylated protein form) and 15 µg (EGFR) of the total protein lysate was dissolved in sample buffer [Laemmli with 5% (v/v) 2-β-mercaptoethanol and 5% (v/v) bromophenol blue and boiled for 5 min at 95ºC.

Following, the proteins were separated by electrophoresis in SDS-PAGE gels with 8% acrilamide and 10% SDS. The human epidermal growth factor receptor (EGFR) and its phosphorylated form weight approximately 132 KDa, being better resolved in a less thick acrilamide. The resulting SDS-PAGE gel was electrically transferred to a nitrocellulose membrane (RTA Transfer Kit, BioRad), using a Trans-Blot® Turbo Transfer System (BioRad) and applying the manufacturer's instructions. After blocking the non-specific binding sites for 1 h with 5% (w/v) not-fat dry milk in PBS-tween-20 (for the non-phosphorylated protein form) and with 5% (w/v) BSA (for the phosphorylated protein form), the membranes were incubated in an agitator overnight at 4°C with different primary antibodies (anti-EGFR diluted 1:500 in 5% non-fat milk, anti-pEGFR-Y^{1068} diluted 1:500 in 5% BSA and anti-GAPDH diluted 1:1000 in 5% non-fat milk buffer).

In the next day, the membranes were washed three times with PBS tween-20 (0.5% v/v) for 5 min and probed with the appropriated secondary antibody, conjugated with horseradish peroxidase [anti-rabbit (sc-2354, Santa Cruz Biotechnology), EGFR, and its phosphorylated form, diluted 1:2000 in 0.5% PSB tween-20, and anti-mouse (sc-2005, Santa Cruz Biotechnology) for GAPDH at room temperature for 1 h, in an agitator. After washed, the membranes were revealed by adding ECL substrates (Pierce) and capture the chemiluminescence by Fusion Solo (Vilber Lourmat) equipment.

Statistical analysis

For *in vitro* experiments, at least one independent replicate were performed (n=1 to 5 sample/experiment). Experiments performed once were considered preliminary results. For, GP comparison was calculated by student's t-

test (two tailed distribution, two sample equal variance). For MTT proliferation assays, results were compared by analysis of variance ANOVA (using GraphPad Prism ver 6). Values of $p<0.05$ were considered statistically significant (*: $p<0.05$).

Results and discussion

Cytotoxic effect of azurin and derived peptides on cancer cells

MTT proliferation assays demonstrated that CT-p26 appears to be at least 10% more active against breast cancer cells (MCF-7) than azurin itself, in the same concentrations (100 µM). Also, p28, another azurin tailored peptide, appears to be 10 to 15% less cytotoxic than CT-p26 against both lung and breast cancer cells (A549 and MCF-7 respectively), also in the same concentration of 100 µM (data not presented). These results are the foundation of this work and primary objective of re-designing the C-terminal extremity of azurin, which comprises CT-p26, with the aim of decreasing its length, improving its solubility and anticancer effect.

In silico optimization of CT-p26

Computational study of CT-p26

In this *in silico* study we aimed for the improvement of CT-p26 with three objectives: increase its anticancer score, shortage of its length and improve its solubility.

In studies meant to validate AntiCP algorithm, the peptides with score above 0.90 proved to have anticancer effect *in vitro* and a peptide with score below 0.50 proved to be non-effective (Ghandehari et al. 2015). To our knowledge, besides the tests we performed on CT-p26, no other peptides with scores of specifically 0.76 were previously tested to validate this threshold, so for the further improvement of CT-p26 anticancer potential along with its shortage we decided to aim for values above 0.90, like the references suggest.

Regarding the length change, shortage of sequence in peptides means the decrease of synthesis cost and the increase in the likelihood of reaching its targets within the organisms, as it is suggested that shorter peptides show more anticancer potential and improved selectivity (Harris et al. 2011; Gaspar et al. 2013). The bioinformatic tool AntiCP was operated in order to test the anticancer potential in shorter versions of CT-p26. The principle used was to progressively reduce the number of residues only in the extremities of the sequence until an optimal sequence was attained (with better score, net charge and amphipathicity values). Indeed, a series of modifications were tested and its anticancer potential calculated by the algorithm (data not presented).

The first modification was the removal of the last three residues S-A-L. Alanine and serine are poor hydrophobic amino acids and so their removal was likely to improve hydrophobicity ratio. That region appears to be very poorly conserved amongst the different species, even within the *Pseudomonas* genus thus was logical that the depletion of this region would arise as first option.

Preliminary tests in CT-p26 showed that this peptide had solubility issues when using PBS as solvent. This is a normal consequence of peptides with positive or next to positive net charge. Because the hydrophobic nature of residues confers its overall net charge and influence other characteristics such as pH, the issue that this new improved peptide would not be easily soluble ascended. *In silico* approaches using solubility prediction algorithms were used to forecast this problem.

Innovagen™ website has a peptide solubility calculator which upon the use of the peptide sequence as input will provide as output the water solubility, pH and, if poorly soluble, solvent alternatives. Indeed, the depletion of the three last residues increased its hydrophobicity ratio but did not improve its poor solubility. Nevertheless, we also tested the CT-p26 sequence with minus seven residues (CT-p19) by depleting the first four residues as well, even though they were hydrophobic ones and an optimal score of 0.90 was given as output (data not presented). Finally, with the suggested single substitutions given by the algorithm, anti-CP's score increased to 0.99 and the solubility prediction improved. As a consequence, a new putative peptide with anticancer potential was designed using CT-p26 as template, a peptide derived from *P. aeruginosa's* azurin. As introduced, the designation given was CT-p19LC, because it has 19 residues instead of 26 and the original template comes from the C-terminal extremity of azurin.

Cytotoxic effect of newly designed CT-p19LC on cancer cells

In Figure 1, CT-p19LC reveals to be active against all tested adenocarcinoma cell lines, although, instead of a dose depended behavior, what it seems to be a bell-shaped biphasic cytotoxic behavior is observed. Such behavior was described on other anticancer agents who induce targeted necrosis in cancer cells or related with anti-angiogenic agents (Reynolds 2010; Wong et al. 2015). This result does not add up to the already known dose dependent profile which trends in azurin, p28 and CT-p26 cytotoxic assays, which is impressive considering that CT-p26 is the template of CT-p19LC.

Indeed, in the assays using CT-p26, p28 and reportedly azurin itself (Bernardes et al. 2017 submitted) cell viability decreased upon gradual dose concentration upgrade which leads to the conclusion that the cytotoxicity power of those peptides appear to trigger a dose depended behavior. Also, on CT-p26 and p28 cell viability profiles, cell death seems to stabilize in concentrations near 50 µM (data not presented). In the same conditions, reports of p28 assays confirm the dose dependent cytotoxicity against malignant cells (Yamada et al. 2013). Consequently, both assays in p28 and CT-p26 in MCF-7 demonstrated a very similar cytotoxic profile (data not presented).

With CT-p19LC concentrations near 20 µM, a fifth of the concentrations with maximum effect when using the other peptides, MCF-7 cells registered a viability decrease of about 60%, which represents what appears to be an improvement of effectiveness by 2-fold in comparison with the template peptide and azurin itself. These results suggest that azurin's anticancer potential is not limited to

p28 fragment substantiating the hypothesis that the residues near azurin's C-terminal that compose CT-p26 may also lethally target cancer cells, in an effective way. All in all, *in vitro* assays results show that CT-p19LC represents an improved version of its model CT-p26, validating the algorithm predictions of optimization in anticancer targeting when tested in breast cancer cell line MCF-7. The same degree of apparent anticancer effectiveness was observed in assays performed on human (A549) lung adenocarcinoma cells (Figure 1). With only 25 µM of CT-p19LC lung cell viability decreased more than 40%, which represents 10 to 15% more cell death then the maximum viability decrease caused by azurin and CT-p26

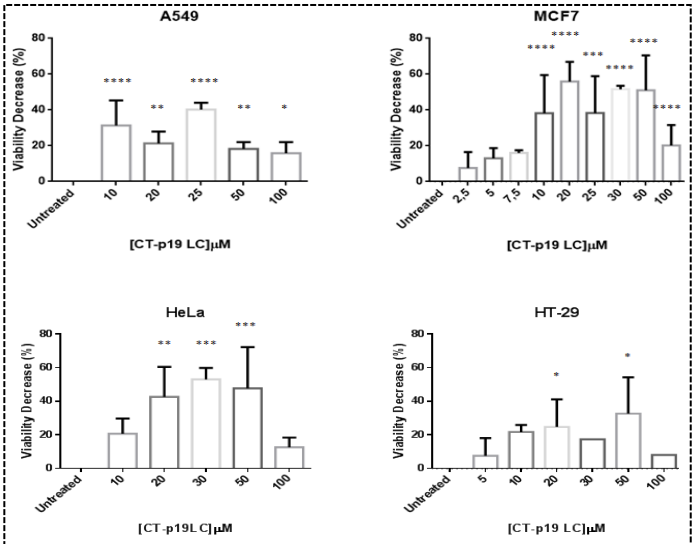

Figure 1| Representation of the effect of CT-p19LC on A549 (lung adenocarcinoma), MCF-7 (breast adenocarcinoma), HT-29 (colorectal adenocarcinoma), and HeLa (cervix adenocarcinoma) cells. These results were obtained by multiple MTT proliferation assays, on each assay every condition was triplicate. The tested concentrations were between the control 0 µM (untreated) and 100 µM. Results were compared to the untreated condition by analysis of variance ANOVA (Newman-Keuls Multiple Comparisons, using GraphPad Prism ver 6). Values of $p<0.05$ were considered statistically significant (*: $p<0.05$).

in A549 cells, and still these data is a representation of concentrations such as 50 and 100 µM, two and four times the concentration used for treatment with CT-p19LC.

On another subject, the implications of the biphasic profile observed in all cell line assays upon treatment with CT-p19LC represent an interesting outline of these assays.

The propositions of these results are only possible to discuss based on the little information that is offered in literature with significant proof of the advantages and/or disadvantages of this pharmacological behavior. In one hand is possible that this apparent biphasic behavior may represent a step back for the anticancer potential of this molecule given that up until very recently the pharmacokinetics of antincancer agents were calculated only based on maximum tolerated dose. The need to calculate effective drug usage considering any other type of behavior other than dose-dependent can still be enough to condemn any new potential anticancer drug in face of risk assessment of the drug regulatory authorities (Calabrese 2004). Indeed, from some time, cancer patients have been regularly treated with chemotherapy drugs at the maximum tolerated dose. According to the threshold dose-response model, this should maximize the chance of eradicating all tumor cells and succumb to the best therapeutic index.

In another hand, some defend that a biphasic profile is not anything but the true profile for the general drugs and that a maximum concentration of effectiveness is not necessarily the highest tolerable. Consequently, instead the dose-response to many drugs may be preferentially modeled using 'hormetic' or 'biphasic' dose-response models (Reynolds 2010).

Hormesis can manifest in several forms: bell-shaped, U-shaped or J-shaped dose-response curves. A bell-shaped dose-response is characterized by low-dose stimulation, followed by loss of this effect at higher doses, as observed Figure 1 with all assays performed on breast, lung, colorectal and cervix adenocarcinoma cell lines. The CT-p19LC effect on these cell lines assumes a bell-shape dose-response where in lower doses CT-p19LC is very bioactive and in higher doses its effect decreases.

Nevertheless, CT-p19LC suffered three point residue alterations and was reduced hence increasing its hydrophobicity. Peptides secondary structures are highly dynamic and easily triggered. Therefore is very possible that by trying to improve membranolytic effect of CT-p26 therefore creating CT-p19LC an alteration on the preferable secondary structures adopted by this peptide occurred.

As such, future re-design of this peptide may be needed if biphasic behavior proves difficult to handle or to extend to more cancer cell lines.

On Figure 1 it is also possible to analyze the assays performed on HeLa (cervix adenocarcinoma) and HT-29 (colorectal adenocarcinoma) cell lines. Although the results of assays performed on HeLa cells resemble the ones already discussed about CT-p19LC effect on A549 and MCF-7, the same does not happen when analyzing HT-29 results. The average LD_{50} of CT-p19LC increases from 20 to approximately 50 µM when compared with results of assays performed on breast and lung cancer cells. The maximum cell viability decrease values were reported to be more than 60% on HeLa cells treated with 50 µM of CT-p19LC and 40% on HT-29 cells treated with CT-p19LC.

These results suggest that HT-29 cells are somehow more resistant to CT-p19LC than MCF-7, A549 and even HeLa cells. Although it is supposed that CT-p19LC mode of action is membrane based its targets may be dissimilar in different types of cancer cells. These differences between cancer cell lines may be the key to unravel this peptide target against human cells. It has been suggested in another work from this group that azurin's 114 residue is important on targeting caveolin (Bernardes et al. 2017 submitted).

The peptide CT-p19LC is designed from that same region containing that same residue which imposes that a putative CT-p19LC interaction with caveolin-1 should be studied in the future. Indeed, it is known that caveolin-1 expression levels differ from cell to cell, and there is no *caveolae* model associated with all cancer cells which means that even within the group of epithelial cancers there may be variances in the caveolin-1 expression pattern (Martinez-outschoorn et al. 2015). Indeed, if CT-p19LC interacts with the lipid rafts of cancer cells then caveolin-1 may be a candidate, but probably not the only one.

CT-p19LC is not effective against breast and lung non-cancer cell lines

In order to test if CT-p19LC shows immediate toxicity against non-cancer cells, two non-malignant cell lines from human lung (16HBE14, bronchial) and from breast (MCF-10A) were treated with different doses of CT-p19LC following an MTT assay to unravel cell proliferation levels (Data not presented). Given that the LD_{50} of CT-p19LC calculated in the assays performed on both A549 and MCF-7 (Figure 1) were the same, around 20 µM, it seemed important to study the effect of that same concentration on the non-cancer cell lines from the same type of tissue.

This preliminary analysis on CT-p19LC effect on non-malignant cells showed very promising results (Data not presented). Despite the apparent cytotoxic effect against the lung cancer cell line A549, assays on normal lung cells registered little toxicity when treated with CT-p19LC, attaining less than 15% of cell viability decrease. The same happened in the assay performed on breast cancer cell line MCF-10A. Less than 10% of cells lost their viability, which is not considered a significant cytotoxic effect. Thus, this preliminary result suggests that we may be in the presence of an ACP_{AO}, although more repetitions and extension to more non-cancerous cell lines should be performed in the future.

CT-p19LC decreases the membrane order of cancer cell lines

The important questions asked more frequently are what are ACP_{AO} (the specific type of anticancer peptides that do not target mammalian healthy cells) mode of targeting cancer cells and on which cancer cell section or internal compartments do they operate against. As introduced before, the majority of action happens on the membrane basis. Therefore, it would be significant to verify the effects of CT-p19LC at the level of the membrane order. To do so, the order of the plasma membranes after treatment with the CT-p19LC peptide was investigated with the probe Laurdan using confocal microscopy in lung (A549), breast (MCF-7), colorectal (HT-29) and cervix (HeLa) adenocarcinoma cell lines. Consequently these cells were treated only with 20 µM which is the concentration of CT-p19LC we consider had the major impact in the MTT assays (Figure 1).

In order to quantify the degree of lipid packing (GP value) in all cell lines and in both conditions (untreated and treated with 20 µM of CT-p19LC), a software based on a MATLAB

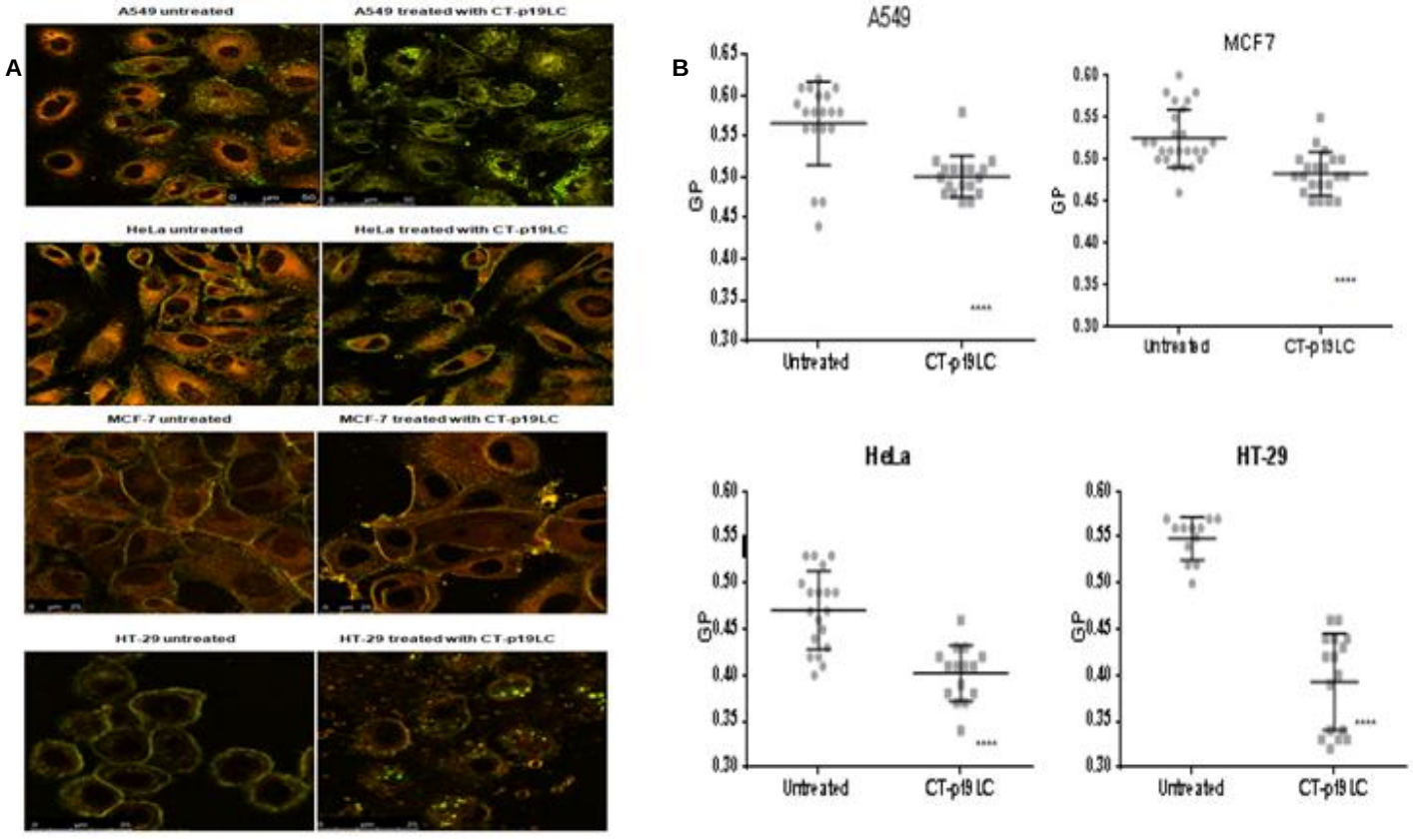

Figure 2| A) Images of confocal microscopy of the impact of CT-p19 on the membrane fluidity of cancer cell lines MCF-7, A549, HeLa and HT-29 taken as described in Material and Methods. **B)** The effects of CT-p19LC in the cell's membrane order of A549 lung cancer cell line, MCF-7 breast cancer cell line, HT-29 colorectal cancer cell line and HeLa cervix cell line and their respective GP values. All represented cell lines were seeded on µ-Slide glass 8 well glass bottom chambers and treated with 20 µM of CT-p19LC for 2h. For each condition 5 µM of Laurdan were used. Untreated cells were the control. Software based on a MATLAB environment was used to measure the GP values. Average GP values are expressed as mean ±SD from at least 15 individual cells in each condition. Results were compared by student's t-test two tailed distribution, two sample equal variance (****: p<0,0001).

environment was used (provided by Dr Fábio Fernandes, CQFM, IN). The GP value varies between -1 and 1, and higher the value the higher is the ordered content of the cells. A GP ≥ 0.5 tells us that we are in the presence of a gel phase, in other words a GP≥ 0.5 correspond to a very compact and ordered content. Below that level, we are in the presence of a more fluid phase (Owen et al. 2011; Pinto et al. 2013).

As we can see in Figure 2A, treated cells from all cell lines suffered a variety of morphological modifications. The cell shape became irregular and the fragmentation of the plasmatic membrane and the nucleus was visible. In Figure 2B, we can see that untreated A549 cells have an average GP of 0,56, meaning that these cells' membranes are considered ordered. When A549 cells were treated with CT-p19LC, a significant decrease in the GP value (0.56 to 0.51) was observed when compared with the untreated cells, meaning that the ordered content of the cells decreases after CT-p19LC treatment. The same pattern is observed in the tests performed on the other cell lines. Untreated MCF-7 breast cancer cells have an average GP of 0,53 which means the membranes are in the gel phase but upon treatment with CT-p19LC average GP decreases to 0,48, a value which indicates the membranes are in the fluid phase.

The peptide CT-p19LC has decreased GP average of cervix cancer cells (HeLa) from 0,48 to 0,40. These results suggest that these cells do not have a high content of ordered domains in their structure. There is no pattern among cancer cells related to their *caveolae* levels, even within the adenocarcinoma types there are variations regarding membrane fluidity and lipid rafts (Martinez-outschoorn et al. 2015). Nevertheless, when we treated HeLa cells with CT-p19LC, the GP obtained was 0.40. Like the other cancer cells' results, a decrease in the ordered domains was observed after CT-p19LC treatment, meaning that this peptide appear to able to decrease the ordered domains of all these adenocarcinoma cell lines. (Singh et al. 2003; Pang et al. 2004)

The most drastic effect observed in cell membrane order with this methodology was when treating HT-29 colorectal cancer cells with CT-p19LC. Untreated cells have an average GP of 0,55, a value that suggests the membrane components are ordered and compact but upon treatment with CT-p19LC for only two hours this value decreased to 0.40 which means the membranes of these cancer cells became very fluid. This result seems to be in conflict with MTT assay results presented on Figure 1, where HT-29 appeared to be slightly more resistant to CT-p19LC in contrast with the other adenocarcinoma cell lines. However, we do not still fully understand CT-p19LC action and although its design and preliminary cytotoxic results may lead to the assumption that we are in the presence of a membranolytic peptide, we still do not know which components this peptide targets. For now, the GP results might indicate that CT-p19LC interacts in some way with lipid rafts but as introduced there are different types of lipid rafts, more specifically there are non-planar lipid rafts and planar lipid rafts. In fact, HT-29 cells are more prone to form planar lipid rafts in contrast with the other adenocarcinoma cell lines in study, which are richer in non-planar lipid rafts.

This membrane order assay reveals that these four adenocarcinoma cell's membranes are highly disturbed upon CT-p19LC treatment in very small doses (20 μM) for a very short time (2 h) which may lead to the conclusion that this peptide's target it is in fact part of these cells membranes adding that lipid rafts constituents are good candidates, including caveolin-1. But the mode of action regarding what caused these cells lethality levels observed in Figure 1 still remains a mystery and may or may not be related to the plasmatic membrane given that internal processes are also a possibility such as apoptosis. For future studies, other biophysical approaches such as AFM or leakage studies using model membranes (liposomes) would be significant to unravel CT-p19LC mode of action against cancer cells.

Treatment with CT-p19LC in combination with erlotinib potentiates the anticancer effect of this agent in lung cancer cell line A549

Erlotinib is a chemotherapeutic agent which targets EGFR. This receptor is of major relevance in lung cancer therapy. In order to invade the surrounding tissues, tumor cells need to adhere to the extracellular matrix (ECM). These events of cell adhesion are possible due to the presence of cell-surface receptors such as the integrin superfamily. Integrins are able to promote the intracellular signaling of other membrane proteins such as Growth Factor (GF) receptors. It has been recently demonstrated that in lung cancer cells β1 integrin controls Epidermal Growth Factor receptor (EGFR) signaling and tumorigenic properties suggesting that this transmembrane protein may be a suitable target for therapies (Howe et al. 2016).

Given the fact that CT-p19LC is derived from azurin and that the effect of this peptide on A549 lung cancer cells appears to be higher than azurin's effect (Figure 1) it was relevant to study the possibility of synergy between CT-p19LC and erlotinib upon exposure on this cell line. This synergy phenomenon is when the effect of the drugs combined is higher than the arithmetic sum of their solo effect (Preet et al. 2015).

In Figure 3, results suggest that CT-p19LC may influence the effect of the drug treatment in cell death. When treating A549 cells with both drugs, if no synergy occurred it was expected that the effect was a viability decrease of 35% or less, however, a viability decrease of almost 50% was observed, which represents an upgrade of 15-20% on drug effect (red). This result strongly suggests that CT-p19LC enhances erlotinib effect. Collectively, both drugs in small doses (LD_{20} or less) upgrade effects reaching a LD_{50} concentration.

Synergy is also observed in results from joint treatment of erlotinib at concentration of 0.5 μM with CT-p19LC at concentration of 20 μM, although not so evident (Figure 3).

A possible hypothesis to explain this synergistic effect could be that CT-p19LC, similarly to azurin, affects, at least in part, the signaling pathways related to *caveolae* and EGFR which is targeted by erlotinib.

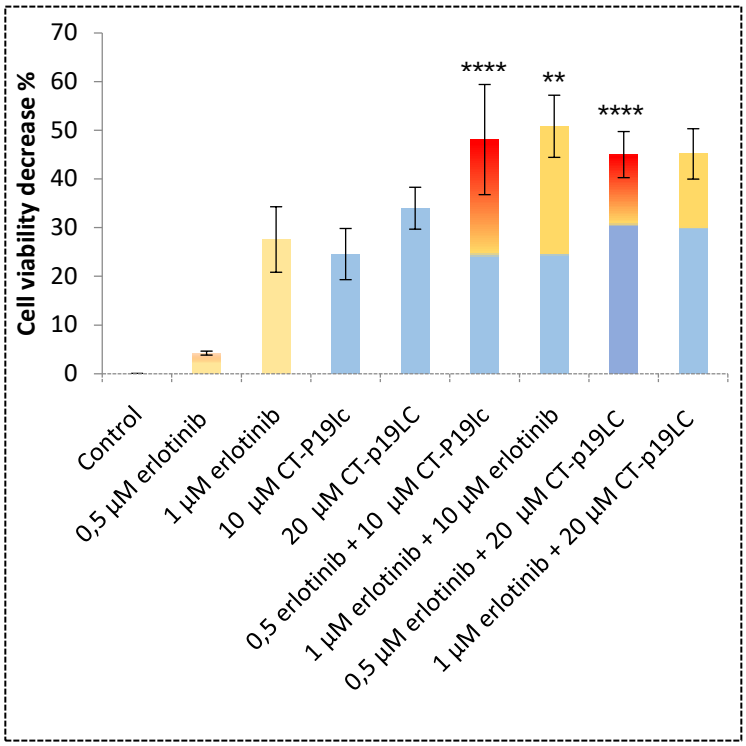

Figure 3| CT-p19LC potentiates the effects of erlotinib. Cells were seeded at a density of 4x103 A549 cells per well was performed in 96-well plates and left to adhere overnight. In the next day, cells were treated CT-p19LC (10 µM and 20 µM), erlotinib (0,5 µM and 1 µM) or a combination of both. After 72h, cell proliferation was determined by MTT assay. Results are expressed as percentage of cell death relative to the control (untreated cells). Values of A549 cell viability decrease are presented as mean + SD. Yellow represents effect of erlotinib only, blue represents effect of CT-p19LC only, and red represents the percentage of viability decrease which goes beyond the sum of the effects of CT-p19LC and erlotinib combined. Results were compared to erlotinib's solo values by analysis of variance ANOVA using GraphPad Prism (ver 6). (**: p<0,01).

Previous results (Bernardes et al. 2017, submitted) suggests that azurin enhance paclitaxel and doxorubicin cytotoxic effect on MCF-7, HT-29 and A549 human cancer cell lines. These results were acquired after these adenocarcinoma cells were exposed to 25, 50 and 100 µM of azurin together with 0.1, 1 and 10 nM of paclitaxel or 0.1, 0.5 and 1µM of doxorubicin during 72 hours. With this study Bernardes et al. were capable of observing that the cell death caused by the combination of both drugs was much higher than the cell death caused by the each substance used independently. Another study of our group also revealed that upon exposure of azurin with gefitinib in lung cancer cells A549, there was a higher decrease in β_1 integrin levels in contrast with exposure to either of the agents alone. This result is rather relevant given the fact that the overexpression of β_1 integrin in lung cancer has itself been associated to the resistance to the treatment with gefitinib, a process that is at least in part mediated by the signaling pathways that are attenuated by azurin. In this study the synergistic effect is evident by an increase of about 15-20% in lung A549 cell death when compared to the sum of the solo cytotoxic effect of azurin and gefitinib. Also, the same result was observed when erlotinib tested in combination with azurin. An identical synergistic behavior was demonstrated by a decrease of 10% in cell viability in comparison with the effect of the single agents, azurin and erlotinib (Bernardes et al. 2016).

Nevertheless, one may not forget that CT-p19LC is *per se* capable of cell death and membrane disorder as evidence was already presented. Consequently, there may be other possible mechanisms that CT-p19LC may interfere with, not contributing directly to cell death, which may increase the efficiency of other agents.

Indeed, it is widely implicit that, although chemotherapy and radiotherapy remain the most common non-surgical cancer treatment options, they present major drawbacks. Consequently, it is imperative to develop new therapeutic strategies, more effective in killing cancer cells but also more selective so the toxic side effects associated to administration of anticancer drugs can be attenuated, if not eradicated.

Conclusions and future perspectives in cancer therapy

CT-p19LC design and anticancer potential explored in this work may represent a relevant enforcement to the relevance of azurin as an anti-tumorogenic protein. Again, a new portion of this protein was used as template for design of a new synthetic peptide which appears to be cytotoxic against four different adenocarcinoma cell lines. Unlike p28, this peptide suffered three residue modifications from the original template with the goal of enhancing tits anticancer potential and gain specificity towards malignant cells through changes in hydrophobicity and net charge. The results from this work suggest that, indeed, CT-p19LC incites higher loss of viability in lung and breast cancer cells in comparison with azurin and p28. It is also bioactive against colorectal and cervix cancer cell lines.

Adding, the results from this work have shown evidence that CT-p19LC, like azurin, has a deleterious effect on membrane order of these four adenocarcinoma cells. Weather this represents an impair effect on caveolae and EGFR on lung cells as it was demonstrated previously from past work of this group to occur when treating these cells with azurin and gefitinib or erlotinib (Bernardes et al. 2016) it remains to be proved. It is also possible that CT-p19LC effect on cancer cells membranes is toxic enough to potentiate the effect of other drugs, such as erlotinib. It would be relevant to study CT-p19LC mode of action in the future. Also, it would be significant to perform more assays to determine CT-p19LC specificity towards more non-cancer cell lines besides human breast and lung cell lines so this peptide specificity properties could be further explored, being one of the most attractive characteristics it seem to present.

Also, the enhanced effect observed to exist when lung A549 cancer cell treatment included both CT-p19LC and erlotinib provides significant conclusions. Synergy between two drugs means that it is possible to upgrade the toxic effect against cancer cells while diminishing the toxic effect the drugs have on healthy cells, by decreasing their concentration. It is not unheard of that some anticancer peptides have been conjugated with known chemotherapeutic drugs, in smaller doses than normally administrated, and proved to be more effective in clinical trials. For instances, the anticancer peptide romidepsin is a FDA approved anticancer agent against T-cell lymphoma

when used alone. Although very effective against hematological tumors, its efficacy was always less significant against solid tumors. Currently, the potential action of this peptide against breast cancer in synergy with Abraxene® (paclitaxel albumin-stabilized nanoparticles) is being tested in humans (NCT01938833). Initially developed to avoid the toxicities associated with polyethylated castor oil, the novel neoadjuvant agent Abraxene® have already proved in a serial of clinical trials recently reviewed by Zong et al. to be an effective solo cytotoxic drug in chemotherapy for primary breast cancer patients, especially in aggressive subtypes (Zong et al. 2017).

Consequently, a nanoparticle containing erlotinib could be decorated with CT-p19LC and its efficacy studied in the future, not only regarding potential cytotoxicity against lung cancer but also hopefully providing data regarding their specificity and promoting drug delivery fine-tuning.

Finally, further studies into this emerging field of anticancer peptides need to be embraced. More *in vitro* studies need to be conducted correlating with the effects reported on numerous cancer cell lines. Understanding the detailed and precise mechanisms of this class of agents and structure-activity relationship will provide a knowledge platform to respond to some unanswered questions about both anticancer and antimicrobial peptides which will most possibly allow the design of superior agents. Instability and degradation of the peptides need to be further studied in order for these agents to exert their full therapeutic potentials and perhaps decipher some activities unknown in the present days

Acknowledgments

Funding received by iBB-Institute for Bioengineering and Biosciences from FCT (UID/BIO/04565/2013) and from Programa Operacional Regional de Lisboa 2020 (Project N.007317) is acknowledged (iBB/2015/12 and IBB/2015/16).

References

Bernardes, N. et al., 2016. Modulation of membrane properties of lung cancer cells by azurin enhances the sensitivity to EGFR-targeted therapy and decreased β1 integrin-mediated adhesion. *Cell Cycle*, 15(11), pp.1415–1424.

Calabrese, E.J., 2004. Hormesis: a revolution in toxicology, risk assessment and medicine. *science & society*, 5, pp.37–40.

Fialho, A.M., Bernardes, N. & Chakrabarty, A., 2016. Exploring the anticancer potential of the bacterial protein azurin. *AIMS Microbiology*, 2(3), pp.292–303.

Gaspar, D., Salomé Veiga, A. & Castanho, M.A.R.B., 2013. From antimicrobial to anticancer peptides. A review. *Frontiers in Microbiology*, 4(OCT), pp.1–16.

Ghandehari, F. et al., 2015. In silico and in vitro studies of cytotoxic activity of different peptides derived from vesicular stomatitis virus G protein. *Iranian Journal of Basic Medical Sciences*, (18), pp.47–52.

Harris, F. et al., 2011. On the selectivity and efficacy of defense peptides with respect to cancer cells. *Medicinal Research Reviews*, 29(6), pp.1292–1327.

Hoskin, D.W. & Ramamoorthy, A., 2008. Studies on anticancer activities of antimicrobial peptides. *Biochimica et Biophysica Acta - Biomembranes*, 1778(2), pp.357–375.

Howe, G.A. et al., 2016. Focal Adhesion Kinase Inhibitors in Combination with Erlotinib Demonstrate Enhanced Anti-Tumor Activity in Non-Small Cell Lung Cancer. *Plos one*, pp.1–20.

Leuschner, C., 2005. Targeting Breast and Prostate Cancers Through Their Hormone Receptors. *Biology of Reproduction*, 73(5), pp.860–865.

Li, Y.C. et al., 2006. Elevated levels of cholesterol-rich lipid rafts in cancer cells are correlated with apoptosis sensitivity induced by cholesterol-depleting agents. *The American journal of pathology*, 168(4), pp.1107-18–5.

Martinez-outschoorn, U.E., Sotgia, F. & Lisanti, M.P., 2015. Caveolae and signalling in cancer. *Nature Publishing Group*, 15(4), pp.225–237.

Owen, D.M. et al., 2011. Quantitative imaging of membrane lipid order in cells and organisms. *Nature Protocols*, 7(1), pp.24–35.

Pang, H., Le, P.U. & Nabi, I.R., 2004. Ganglioside GM1 levels are a determinant of the extent of caveolae / raft-dependent endocytosis of cholera toxin to the Golgi apparatus. *Journal of Cell Science*, (117), pp.1421–1430.

Pinto, S.N. et al., 2013. A combined fluorescence spectroscopy , confocal and 2-photon microscopy approach to re-evaluate the properties of sphingolipid domains. *BBA - Biomembranes*, 1828(9), pp.2099–2110.

Preet, S. et al., 2015. Effect of nisin and doxorubicin on DMBA-induced skin carcinogenesis — a possible adjunct therapy. *Tumor Biology*.

Punj, V. et al., 2004. Bacterial cupredoxin azurin as an inducer of apoptosis and regression in human breast cancer. *Oncogene*, 23(13), pp.2367–78.

Reynolds, A.R., 2010. Potential relevance of bell-shaped and u-shaped dose-responses for the therapeutic targeting of angiogenesis in cancer. *Dose-Response*, 8(3), pp.253–284.

Sanchez-Navarro, M., Teixido, M. & Giralt, E., 2017. Jumping Hurdles: Peptides Able To Overcome Biological Barriers. *Accounts of Chemical Research*, (50), pp.1847–1854.

Singh, R.D. et al., 2003. Selective Caveolin-1 – dependent Endocytosis of Glycosphingolipids. *Molecular Biology of the Cell*, 14(August), pp.3254–3265.

Teixeira, V., Feio, M.J. & Bastos, M., 2012. Role of lipids in the interaction of antimicrobial peptides with membranes. *Progress in Lipid Research*, 51(2), pp.149–177.

Wong, D.Y.Q., Lim, J.H. & Ang, W.H., 2015. Induction of targeted necrosis with HER2-targeted platinum(IV) anticancer prodrugs. *Chem. Sci.*, 6, pp.3051–3056.

Yamada, T. et al., 2013. p28, A first in class peptide inhibitor of cop1 binding to p53. *British Journal of Cancer*, 108(12), pp.2495–2504.

Yamada, T. et al., 2004. Regulation of Mammalian Cell Growth and Death Relevance by Bacterial Redox Proteins. *Cell Cycle*, 3(June), pp.752–755.

Zong, Y., Wu, J. & Shen, K., 2017. Nanoparticle albumin-bound paclitaxel as neoadjuvant chemotherapy of breast cancer : a systematic review and meta- analysis. *Oncotarget*.